Nuclear Instruments and Methods in Physics Research B 267 (2009) 37–44

Contents lists available at ScienceDirect

Nuclear Instruments and Methods in Physics Research B

journal homepage: www.elsevier.com/locate/nimb

New Geant4 cross section models for PIXE simulation

H. Ben Abdelouahed [a,*], S. Incerti [b], A. Mantero [c]

[a] Centre National des Sciences et Technologies Nucléaires (CNSTN), Pôle technologique, 2020 Sidi Thabet, Tunis, Tunisia
[b] Université Bordeaux 1, CNRP/IN2P3, Centre d'Etudes Nucléaires de Bordeaux-Gradignan (CENBG), 33175 Gradignan Cedex, France
[c] Istituto Nazionale Fisica Nucleate (INFN), Sezione di Genova, Via Dodecaneso 33, 16146 Genova, Italy

ARTICLE INFO

Article history:
Received 16 June 2008
Received in revised form 29 October 2008
Available online 3 December 2008

PACS:
78.20.Bh
78.70.-g
78.70.En
79.20.Ap

Keywords:
Geant4 simulation toolkit
PIXE
Ionisation cross sections
ECPSSR

ABSTRACT

We have implemented in the Geant4 simulation toolkit a set of new ionisation cross sections for the simulation of particle induced X-ray emission (PIXE), based upon theoretical and semi-empirical models. The set provides a model based on the so-called ECPSSR theory for the computation of K-shell ionisation cross sections for proton and alpha particle impact. A second model is based upon semi-empirical expressions proposed by Orlic for the calculation of L_i-subshells ionisation cross sections for proton impact. Our developments are compared to ionisation cross sections already existing in the Geant4 toolkit and to experimental data.

1. Introduction

Among various ion-beam techniques, like charged particle activation (CPA), prompt nuclear reaction analysis (NRA) or particle-induced X-ray emission (PIXE), the later one is certainly playing the leading role [1]. Its multi-elemental character and the fact that PIXE is most suitable for analysis of trace elements of medium and high atomic number in a matrix composed of light elements, make PIXE the most useful technique in environmental, biological and medical applications [2]. During the last decade, PIXE has been accepted by the analytical chemistry community as a standard method for quantitative elemental analysis [3]. However, taking into account that the method involves a particle accelerator, operated by experienced staff and a complex system of detectors and related techniques, the simulation of a PIXE experiment is particularly helpful and even required to reach a sufficient level of precision for signal and background.

Monte Carlo methods are well adapted to the simulation of PIXE, since they can reproduce the stochastic behaviour of the emission process. Today, several Monte Carlo toolkits are available for the simulation of particle interaction with matter, like the widely used Geant4 [4,5], MCNP [6], Penelope [7] and EGS4 [8] codes. Among the four-cited, Geant4 has a very flexible design: it is based on the object-oriented technology [9] and follows an iterative-incremental software process [10], allowing its extension and refinement without disturbing the existing user code.

This work aims to extend the Geant4 toolkit [11] for PIXE simulation by implementing new models for the calculation of the atomic ionisation cross sections of K-shells and L_i-subshells induced by protons and alpha particles. These new cross section models are first described and then are tested through a comparative study involving a collection of reference cross section values. The experimental validation of the PIXE modelling based on these new cross sections will be the subject of another paper.

2. PIXE simulation in Geant4

The Geant4 toolkit is able to model electromagnetic physics processes down to a lower limit of 250 eV thanks to the Low Energy Electromagnetic Package [12], in particular to address requirements of interest for medical [13] and space science applications [14,15]. Modelling the PIXE process in Geant4 requires to model atomic ionisation followed by atomic de-excitation. In the case of incident photons, cross sections for the photoelectric effect associated to each atomic shell or subshell are calculated from the EPDL97 (evaluated photons data library) data library [16]. For electrons, the ionisation cross sections are calculated from the EEDL

* Corresponding author. Address: Centre National des Sciences et Technologies Nucléaires (CNSTN), Pôle technologique, 2020 Sidi Thabet, Tunis, Tunisia. Tel.: +216 21091877; fax: +216 71537555.
E-mail address: habdelou@cern.ch (H. Ben Abdelouahed).

0168-583X/$ - see front matter © 2008 Elsevier B.V. All rights reserved.
doi:10.1016/j.nimb.2008.11.025

Table 1
Geant4 existing model based on separate fitting functions [21].

	Low incident protons	High incident protons
$6 \leqslant Z \leqslant 25$	$x^a e^{b-cx}$	$ab^{1/x} x^c$
$26 \leqslant Z \leqslant 35$	$ab^{1/x} x^c$	3 Logarithmic order
$36 \leqslant Z \leqslant 65$	$ab^{1/x} x^c$	$ab^{1/x} x^c$
$66 \leqslant Z \leqslant 92$	$ab^{1/x} x^c$	4 Logarithmic order

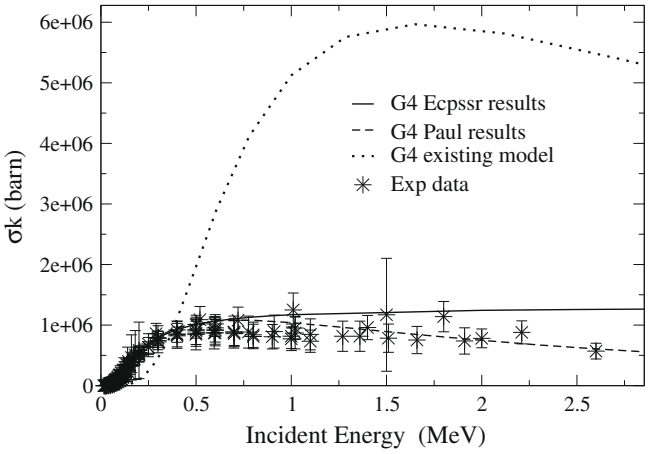

Fig. 1. K-shell ionization cross section by protons impact of element $Z_2 = 6$.

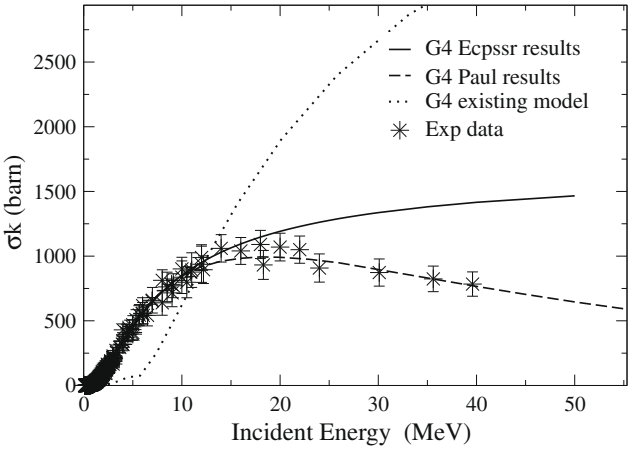

Fig. 2. K-shell ionization cross section by protons impact of element $Z_2 = 29$.

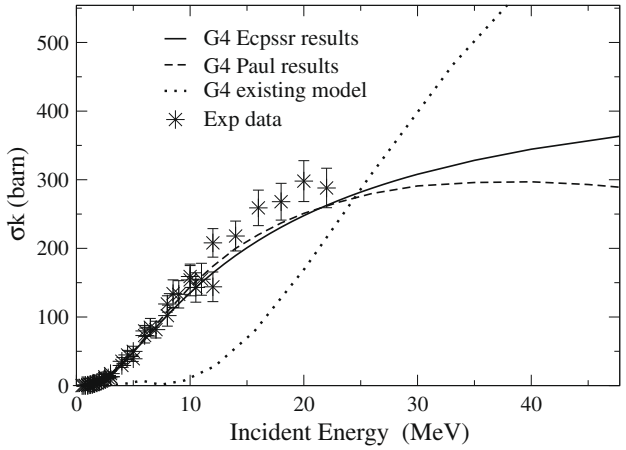

Fig. 3. K-shell ionization cross section by protons impact of element $Z_2 = 39$.

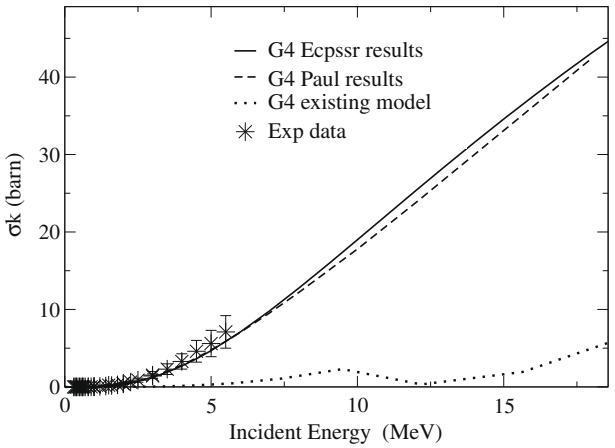

Fig. 4. K-shell ionization cross section by protons impact of element $Z_2 = 51$.

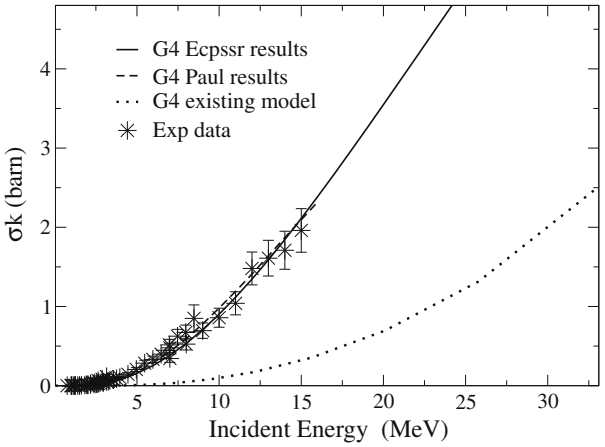

Fig. 5. K-shell ionization cross section by protons impact of element $Z_2 = 73$.

(evaluated electrons data library) data library [17]. The simulation of atomic de-excitation [18] uses the EADL (evaluated atomic data library) data library. This library provides electron binding energies for all subshells, transition probabilities between subshells for fluorescence and Auger emission, as well as energies of the emitted photon or electron. It applies to elements with atomic number between 6 and 92 [19].

The first implementation of PIXE process modelling available in Geant4 was based on the Gryzinski theoretical model [20] and showed a lack of accuracy [21,22].

Another implementation was then proposed by Mantero et al. in the Geant4 Low Energy Electromagnetic Package [18], limited to the modelling of PIXE from K-shell ionisation by incident protons. The cross sections are calculated by using an empirical model implemented in the *G4hshellCrossSectionExp* and *G4hshellCrossSectionExpData* classes. A somewhat arbitrary division of atomic species in four groups was adopted to account for the energy variation of the K-shell cross sections and a separate fit was performed for each group and for low and high energy of incident protons. We report in Table 1 the fitting functions used. K-shell cross sections computed with this existing model are denoted as "G4 existing model results" from Figs. 1–5.

3. Innovative aspects of the proposed development

In the presented work, we have proposed to improve and extend to other incident particles the computation of ionisation cross

sections for PIXE modelling. We have first implemented a new cross section computation based on the ECPSSR theory for K-shell ionisation, both for incident protons and alpha particles. We have then implemented the calculation of ionisation cross sections for L_i-subshells.

K-shell ionisation cross sections can be calculated theoretically with quite high confidence for a wide range of incident particle energies and almost all target atomic numbers. For L_i-subshells, the situation is less favourable, because the available experimental L-subshell data are still rather scarce. In a number of recent reviews [24–26] the authors tried to assess the reliability of experimental L_i-subshell cross section data and compared them with values calculated by using different theoretical models. According to them, predictions for L_i-subshell ionization cross sections agree with the experimental data within 50–60% only. Discrepancies reach an order of magnitude for heavy projectiles at low energies. Consequently, much care and further polishing of theoretical models for L_i-subshell ionisation cross sections are needed before trying to adopt one of them.

4. K-shell ionisation cross section

4.1. Existing theoretical models

Three theories have been refined in attempt to better explain experimental values of K-shell ionisation cross sections:

- The classical approach, the binary encounter approximation (BEA) of Thomson [27] revised by Mantero [21] and reviewed by Lapicki [28].
- The semi-classical approach (SCA) of Bang and Hansteen [29].
- The quantum mechanical plane-wave born approximation (PWBA) of Lewis and Merzbacher [30].

Numerical, analytical and semi-empirical approaches for calculation of K-shell ionisation were derived from those cited models by applying various corrections taking into consideration multiple physical effects such as binding, polarisation, relativistic and deflection effects [31–34].

4.1.1. Semi-classical approach (SCA)

The theoretical hydrogenic model was applied by Smit based on the SCA [35]. It takes into account the projectile kinematics in the field of the nucleus and the atomic electrons and the Hartree-Fock field within a simplified coupled-channel approach. The calculation provides cross sections that agree rather well with experimental data in a broad Z and velocity region (for Aluminium, cross sections are systematically 15% below the considered reference values of Paul and Sacher [23]). Nevertheless, we cannot adopt the SCA model because of its limitation to the following criteria given by Bang and Hansteen [29]:

$$\left(\frac{2Z_1Z_2e^2}{\hbar v_1}\right) \gg 1,$$
$$Z_1 \ll Z_2 \quad \text{and} \quad \Delta E/E_1 \ll 1,$$

where the indices 1 and 2 refer to the projectile and target nucleus respectively, v_1 is the initial projectile velocity and $\Delta E = E_B + E_f$ with E_B denoting the binding energy of the Coulomb ejected electron in the initial bound state and E_f the final energy of this electron.

4.1.2. Plane-wave born approximation (PWBA)

In their original work with PWBA, Lewis and Merzbacher [30] proposed a simple correction method to include the relativistic effects by modifying the screening parameter. Their proposed K-shell ionization cross sections were cast as:

$$\sigma_K^{\mathrm{PWBA}}(\xi_k,\theta_K) = (\sigma_{0K}/\theta_K)F_K(\xi_K,\theta_K) \quad \text{with} \quad \sigma_{0K} = 8\pi a_0^2\left(\frac{Z_1^2}{Z_{2K}^2}\right),$$

where a_0 is the Bohr radius, Z_1 is the projectile atomic number and $Z_{2K} = Z_2 - 0.3$ is the effective atomic number of the target atom seen by an electron in the K-shell, Z_2 is the target atomic number, θ_K is the ratio of the observed binding energy to its screened hydrogenic value $\frac{1}{2}v_{2K}^2$ with $v_{2K} = Z_{2K}\cdot\left(\frac{2.Ry}{m_e}\right)$ is the hydrogenic-Bohr velocity of the target-K-shell electron (Ry is the Rydberg constant and m_e is the electron mass). $\xi_K = 2v_1/(\theta_K v_{2K})$ is the scaled velocity were v_1 is the velocity of the projectile and $F_K(\xi_K,\theta_K)$, which was tabulated by Rice et al. [36], is a dimensionless function called the reduced universal cross section. At K-shell level, the scaled velocity ξ_K is less that 1 and the reduced universal cross section starts to be independent of θ_K and can be calculated according to this formula:

$$F_K(\xi_K,\theta_K) = (2^9/45)\frac{\xi_K^8}{(1+1.72\xi_K^2)^4}.$$

Brandt and Lapicki [37] modified the PWBA model by going beyond the first Born Approximation to initiate the ECPSSR theory.

4.1.3. ECPSSR theory

The ECPSSR theory accounts for the projectile's **E**nergy loss and its **C**oulomb deflection from the straight-line trajectory; in addition, this theory considers the inner shell as a **P**erturbed **S**tationary **S**tate using a scaling factor ζ_K and attempts to simulate numerical procedures that employ **R**elativistic wave-functions.

The K-shell ionisation cross sections, according to Brandt and Lapicki [37], can be written, as:

$$\sigma_K^{\mathrm{ECPSSR}} = 9E_{10}\left[\frac{2\pi dq_{0K}\zeta_K}{z_K(1+z_K)}\right]f_K(z_K)\sigma_K^{\mathrm{PWBA}}(\xi_K^R/\zeta_K,\zeta_K\theta_K). \quad (1)$$

The form of the scaling factor ζ_K, describing the binding-polarization effect correction and presented by Cipolla and Liu [38], is given by:

$$\zeta_K(\xi_K) = 1 + \frac{2Z_1}{Z_{2K}\theta_K}(g_K(\xi_K) - h_K(\xi_K)),$$

where $g_K(\xi_K)$ and $h_K(\xi_K)$ are analytical functions that account for the velocity dependence of the correction, $h_K(\xi_K)$ is related to polarization effects on the binding energy due to the presence of the projectile ion in the atom.

The relativistic scaled velocity $\xi_K^R = \left[m_K^R(\xi_K/\zeta_K)\right]^{1/2}\xi_K$ is function of m_K^R which expresses the relativistic target electron mass correction [38]. The energy loss effect is given by the analytical function $f_K(z_K)$ in terms of $z_K = (1-\zeta_K\Delta_K)^{1/2}$ where Δ_K is the minimum fractional energy loss of the projectile during K-shell ionisation; its formula is described by Brandt and Lapicki [37]. The Coulomb deflection of the projectile is taken into account in the Eq. (1) via:

$$E_{10}\left[\frac{2\pi dq_{0K}\zeta_K}{z_K(1+z_K)}\right]$$

which is an exponential–integral function of order 10. $q_{0K} = (E_i - E_f)/v_1$ is the minimum momentum transfer (which is function of the initial E_i and the final E_f kinetic energy of the projectile in the system), $d = Z_1Z_2/Mv_1^2$ is the half distance between the collision partners at closest approach and $M = (M_1^{-1} + M_2^{-1})^{-1}$ is the reduced mass of the system.

4.1.4. Selection of the suitable model

The successful description of experimental data using an analytical expression makes the ECPSSR approximation very convenient for the computation of K-shell ionisation cross sections [39,40]. Cipolla et al. [38,39] have already adopted the ECPSSR theory, using a personal computer, to develop a program – "ISICS" – allowing the calculation of K-, L- and M-shell ionisation cross

sections. Campbell describes his work on K X-rays from pure elements using 3 MeV protons and shows that results produced by ECPSSR and reference data agree at about the 2% level [40]. Such a good agreement led them to introduce the ECPSSR model into their "GUPIX" (package III) to complement its existing theoretical database and which is widely used in laboratories around the world. We consequently chose to implement the analytical expression of σ_K^{ECPSSR} in the Geant4 Low Energy Electromagnetic Package.

4.2. Geant4 implementation of the ECPSSR model

We implemented in Geant4 the ECPSSR model for the computation of the K-shell ionisation cross section in a dedicated class called *G4ecpssrCrossSection*. This class calculates cross sections for all elements from $Z = 4$ to $Z = 92$, for proton and alpha particle impact (cross sections computed with the *G4ecpssrCrossSection* class are denoted "G4 ecpssr results" from Figs. 1–10) and no condition or limit is imposed on the incident energy value to achieve calculation.

4.3. Comparison with reference data

We have verified our Geant4 computation of K-shell ionization cross sections for incident protons [56] and alphas [23], with the semi-empirical model of Paul and Sacher [23]. This reference model is considered today as a reference. A brief description of the model follows.

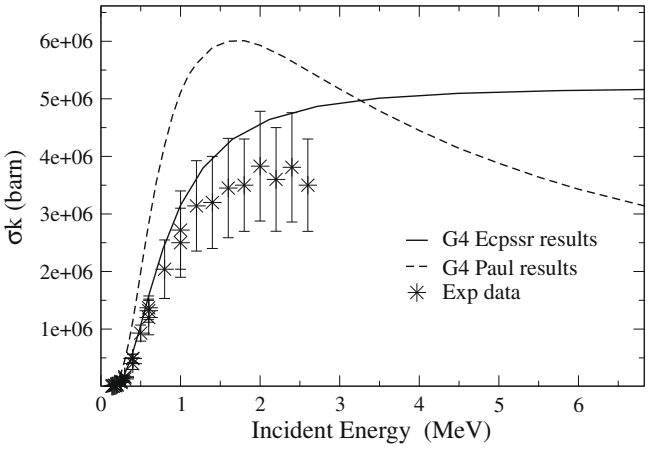

Fig. 6. K-shell ionization cross section by alpha particles impact of element $Z_2 = 6$.

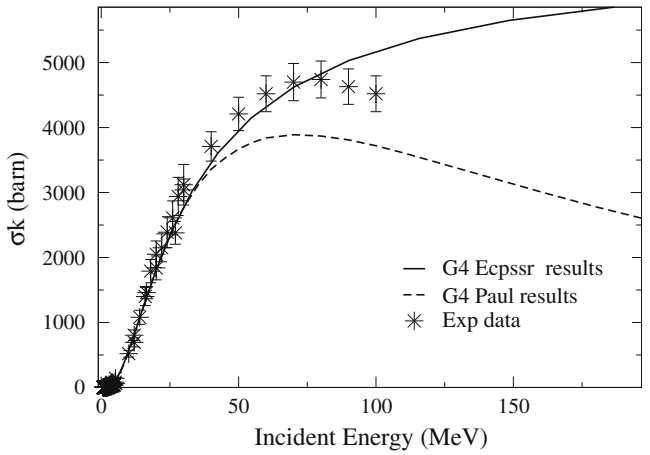

Fig. 7. K-shell ionization cross section by alpha particles impact of element $Z_2 = 29$.

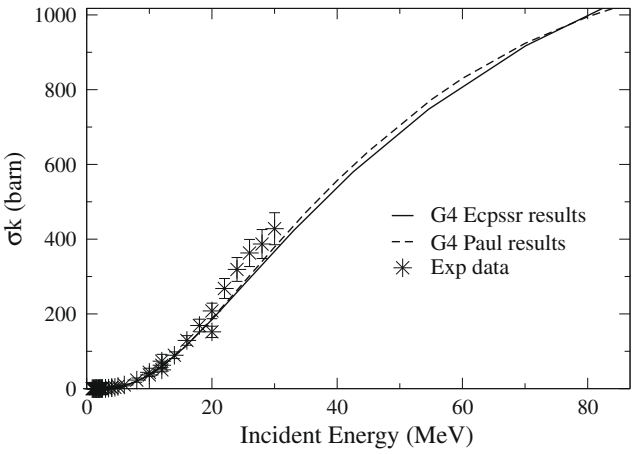

Fig. 8. K-shell ionization cross section by alpha particles impact of element $Z_2 = 39$.

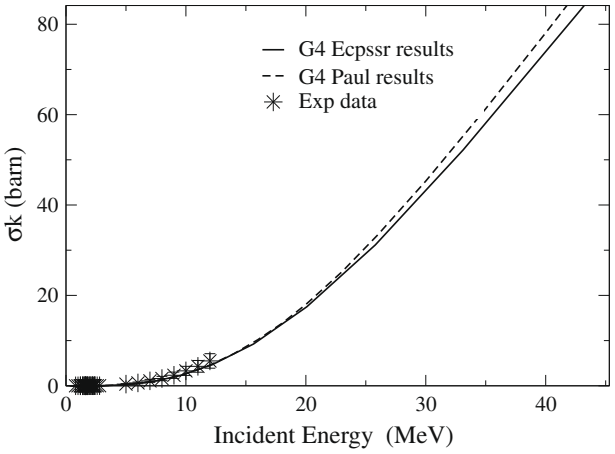

Fig. 9. K-shell ionization cross section by alpha particles impact of element $Z_2 = 51$.

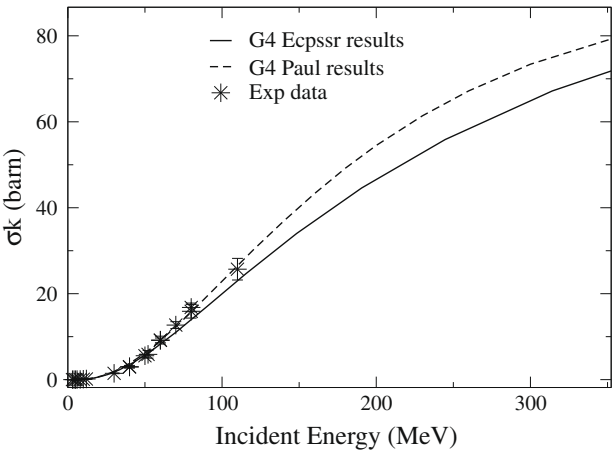

Fig. 10. K-shell ionization cross section by alpha particles impact of element $Z_2 = 73$.

4.3.1. Paul's semi-empirical model

By the use of suitable approximations, researchers have intended to fit experimental collected values to construct a "universal" curve for the calculation of the ionization cross sections of any atomic element at any particle energy. The semi-empirical

function describing that universal curve has to fit to the experimental data and to be in agreement with theoretical predictions. A fifth-order polynomial function was used in many works (Akselsson et al. [41], Johanson and Johanson [42], Romo-Kroger [43]) to attempt to describe the universal curve. In some other works (Paul [44]) a sixth-degree polynomial fitting function was applied to the experimental cross sections, with a relatively good accuracy. Other semi-empirical alternatives proposed by Paul and Sacher presented a statistical analysis of more that 4000 experimental data points for K-shell ionization cross sections by protons impact, reported from about 80 selected publications according to a statistical criterion [23]. Paul and Sacher's approach is based upon examination the ratios (denoted s) of measured cross sections to theoretical ECPSSR cross sections computed by Brandt and Lapicki's work. The s values were considered as functions of the scaled velocity ξ_K of the projectile. The data were grouped into five different ranges of target atomic number, which are treated separately: 4–10; 11–30; 31–40; 41–60; and 61–92. The velocity-range was divided into equal intervals and a weighted average $\bar{s}$ was calculated from the data for each interval. These $\bar{s}$ values were then fitted to a third degree polynomial in order to provide a complete set of $\bar{s}$ values for all relevant energies and atomic numbers.

4.3.2. Implementation of Paul's model for verification

Since Paul's fitting is difficult and time consuming and since fitted data were already available [23,56] from his published work and web site, we downloaded the package and split the data into 88 files corresponding to each element from $Z = 4$ to $Z = 92$. These 88 files were included into the Geant4 data library. A specific class named *G4PaulKCrossSection* was implemented in order to interpolate these rearranged Paul's data. This class is able to reproduce automatically Paul's K-shell ionisation cross sections (called "G4 Paul data" in plots from Figs. 1–10) at any incident energy of protons or alpha particles.

4.4. Results and discussion

Cross section values obtained by the proposed classes (*G4ecpssrCrossSection* and *G4PaulCrossSection*) are plotted, with experimental values extracted from [23,56], as function of projectile incident energy and are presented in figures below. K-shell cross sections for proton impact are shown in Figs. 1–5. We presented results corresponding to five target elements, each one representing one element subgroup ($Z_2 = 6$ from the subgroup [4–10], $Z_2 = 29$ from the subgroup [11–30], $Z_2 = 39$ from the subgroup [31–40], $Z_2 = 51$ from the subgroup [41–60] and $Z_2 = 73$ from the subgroup [61–92]).

Figs. 6–10 show K-shell ionization cross sections for alpha particle impact. We considered the same target elements as for proton impact, in order to visualize the effect of projectile type on K-shell ionisation cross section value for a common target element.

Inspection of K-shell ionization cross section plots (from Figs. 1–10) in both cases of proton and alpha particle impact, shows that Geant4 results given by both implemented cross section models (ECPSSR and Paul's fitting) generally agree with experimental ones. Nevertheless, we noted that the degree of agreement is function of several parameters, which are the atomic number Z_2 of target element and the projectile characteristics (incident energy and particle type).

As it was explained in most of studies [38–40,45,46] dealing with theoretical calculation of K-shell ionization cross sections, for light elements ($Z_2 \leqslant 30$), ECPSSR over-predicts experimental data; the larger the incident energy, the higher the discrepancy (Figs. 2 and 7). This over-estimation is attributed to the fact that ECPSSR theory over-estimates binding effects for decreasing projectile velocity (which is function of target binding energy, target and projectile velocities). This slight breakdown noted on the ECPSSR theory motivated Cipolla [39] to propose the united-atom approximation "UA-ECPSSR". It consists in saturating the binding correction at a value that corresponds to the binding energy of the unified-atom (which means the assembly projectile-nucleus). This improvement has been incorporated into the new version of the ISIICS2006 program [47] for the calculation of ionisation and X-ray production cross sections.

For both cases of proton and alpha particle impact, Paul's reference values obtained from Geant4 for elements $11 \leqslant Z_2 \leqslant 92$ are in agreement with the ECPSSR's ones within 10% for a large band of projectile energy. Since in Paul's fitting method, experimental values are, at first, normalized by ECPSSR ones then averaged and interpolated, it is expected that Geant4-Paul values keep approximately close to Geant4-ECPSSR values.

In the case of alpha particle impact, the degree of agreement between Geant4-ECPSSR, Geant4-Paul and experimental values appears to be the same as in the case of proton impact; its is strongly dependent on the atomic number of the target element and the energy of the projectile. Moreover, divergence between the two Geant4 computation methods (ECPSSR and Paul's) of K-shell ionisation cross section does not exceed 18% with almost all target elements ($31 \leqslant Z_2$) and for both cases of proton and alpha particle impact.

5. L_i-subshell ionisation cross section

5.1. Existing theoretical models

The existing models for L_i-subshell cross sections calculation include:

- The perturbed-stationary-state theory with corrections for energy loss, coulomb deflection and relativistic effects (ECPSSR);
- The binding-encounter approximation taking into account the Binding effect and Coulomb retardation (BEA-BC);
- The semi-classical approximation with binding energy, Coulomb deflection and Relativistic corrections integrated (SCA-BCR).

Those three models have been compared by Cuzzocrea et al. [45,48] to conclude that the BEA-BC theory reproduces on average the magnitude of measured cross sections but often shows different behaviours, being alternatively lower and higher than the experimental data. The SCA-BCR predictions are generally higher than the experimental values. The ECPSSR theory provides the best agreement both for the absolute values and for the overall trend of the experimental cross sections.

A similar comparison was done by Braziewicz et al. [49] between predictions of the ECPSSR and SCA-UA (using united-atom values for the binding energy) theories. Results show that L_i-subshell ionisation cross sections normalized to the ECPSSR and SCA-UA theories have an approximate universal behaviour when they are plotted against the reduced velocity parameter. But both of them systematically over-predict the experimental data for low projectile velocity. For L_1-subshell, the SCA-UA theory does not reproduce the experimental ionisation cross sections. Mukoyama and Sarkadi [50] and Kennedy et al. [51] compared in their works the ECPSSR theory with the Relativistic PWBA theory modified with the Binding energy and Coulomb deflection effects (RPWBA-BC). The RPWBA-BC was found to be in a good agreement with the ECPSSR theory for the low energy region but not for high energy projectiles.

Seeing that the best estimation is generally achieved by using ECPSSR theory, Lapicki [52] tried to improve that theory by applying

various modifications: (i) replacement of the non relativistic screened hydrogenic wave-functions by relativistic Dirac-Hartree-Slater (DHS) ones; (ii) derivation of the perturbed-stationary-state function not in a separated-atom picture but in a united-atom (UA) one; (iii) consideration of redistribution of the vacancies induced by the projectile via intra-shell (IS) transition in the same collision; (iv) a quantum refinement (QC) of the classical Coulomb deflection factor. Predictions of the ECPSSR model with (DHS-UA-IS-QC) and without modifications were then compared with the most recent empirical data from Orlic et al. [53]. Ratios $R_i = \sigma_{\mathrm{Li}}^{\mathrm{exp}}/\sigma_{\mathrm{Li}}^{\mathrm{theory}}$ against relativistic scaled velocity $\xi_{\mathrm{Li}}^{R} = \left[m_{\mathrm{Li}}^{R}(\xi_{\mathrm{Li}}/\zeta_{\mathrm{Li}})\right]^{1/2}\xi_{\mathrm{Li}}$ were plotted and discussed. Plots show that the applied DHS-UA-IS-QC modifications substantially eliminate the large discrepancies and bring agreement for all data within a 50% margin. Nevertheless, Lapicki concluded the impossibility of choosing definitively which theory, ECPSSR or DHS-UA-IS-QC-ECPSSR, is better. Both theories provide reliable cross sections for PIXE packages within the experimental uncertainties of the data. Both of them give essentially the same good results above 1 MeV; they start to differ to a significant extent from the experimental data for projectile energies above several hundred keV. A fitting subsets of Orlic's data [53] measured at 400 keV and below to a polynomial in a single variable as a function of L_i and proton energy shows that ECPSSR overestimate the cross sections measured in the 150–200 keV range by as much as a factor of 12 and the DHS-UA-IS-QC-ECPSSR rises by more than a factor of 16 above the fitted values.

5.2. Existing semi-empirical models: Orlic's model

Discrepancies among experimental values and with theoretical predictions have motivated some authors to fit semi-empirical expressions to the experimental L_i-subshell ionisation cross sections. Sow et al. [54] derived a set of coefficients for calculated L_1, L_2 and L_3-subshell ionisation cross sections for six different groups of target atomic numbers. By using a large number of experimental values, the reliability of the fitted values is significantly improved. The overall reliability of fitted L_i-subshell cross sections is 2–5% for the common proton energies (0.5–4 MeV) and target atomic numbers ($43 \leqslant Z \leqslant 80$) reaching 15% at low energies and high atomic numbers.

In the last work of Orlic et al. [55], empirical data were fitted separately for L_1, L_2 and L_3-subshells. They are split into six subgroups according to their atomic number: $14 \leqslant Z \leqslant 42$, $43 \leqslant Z \leqslant 50$, $51 \leqslant Z \leqslant 60$, $61 \leqslant Z \leqslant 70$, $71 \leqslant Z \leqslant 80$ and $81 \leqslant Z \leqslant 92$. Within each subgroup, between 130 and 500 experimental data points are available, producing quite reliable fitting results. The analytical function used for the fitting is a polynomial function of the following form:

$$\ln(\sigma_i U_i^2) = A_0 + A_1 x + A_2 x^2 + A_3 x^3 + \cdots + A_9 x^9, \tag{2}$$

where $x = \ln[E/(\lambda U_i)]$ is the natural logarithm of the normalized energy $E/(\lambda U_i)$, σ_i is the L_i (i = 1,2,3) subshell ionization cross section in barns, U_i is the L_i subshell electron binding energy in keV, E is the proton energy in keV and $\lambda = 1836.109$ is the ratio of proton mass to electron mass. Coefficients A_0–A_9 of Eq. (2) are obtained by fitting to function to the experimental data points. To reduce the total number of coefficients, experimental data were first fitted with a four-degree polynomial and if the fitting was not good, the degree of polynomial was increased until a satisfactory fitting was obtained. The coefficients obtained and published by Orlic et al. [55] are then used for our ionisation cross section computation in Geant4.

We have to add that at Table 2 of Orlic's work [55] which presents the fitting coefficients for the calculation of L_1, L_2 and L_3-subshell ionisation cross sections, the value corresponding to the coefficient A_5 of L_3-subshell fitting, within the range of target atomic numbers between 41 and 50, should be equal to 0 because there is no need to increase the degree of polynomial to more than the fourth degree, otherwise the fitting function will give wrong results.

5.3. Implementation of Orlis's model

In total, we have introduced 98 fitting coefficients in a dedicated class named *G4OrlicLCrossSection*. This class is able to compute L_1, L_2 and L_3-subshell ionisation cross sections (called "G4 Orlic Li" in plots from Figs. 11–16) corresponding to all elements from Z_2 = 14 to Z_2 = 92.

5.4. Verification

In order to verify the reliability of the cross section computation results produced by our *G4OrlicLCrossSection* class, reference L_i-subshell cross sections are needed. Since no reference data are established, we used the most recent tabulated database [53] which is a continuation of the work of Sokhi and Crumpton [26] and which comprises more than 6000 compiled L_i-subshell cross section values. We present results produced by the *G4OrlicLCrossSection* class and experimental values, for six elements, each one representing one subgroup in the ranges $14 \leqslant Z_2 \leqslant 42$, $43 \leqslant Z_2 \leqslant 50$, $51 \leqslant Z_2 \leqslant 60$, $61 \leqslant Z_2 \leqslant 70$, $71 \leqslant Z_2 \leqslant 80$ and $81 \leqslant Z_2 \leqslant 92$.

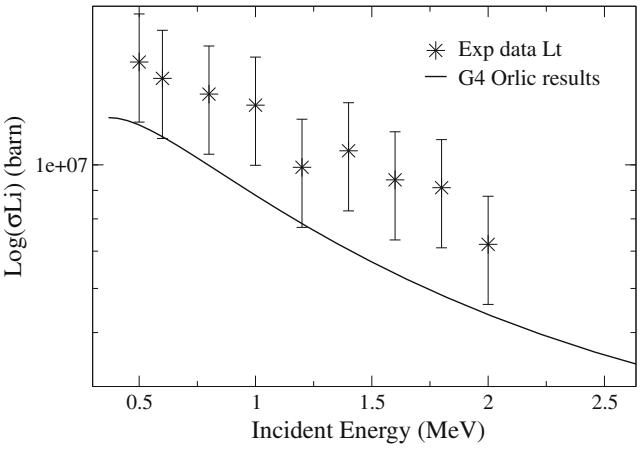

Fig. 11. Total L-shell ionization cross section of element Z_2 = 14.

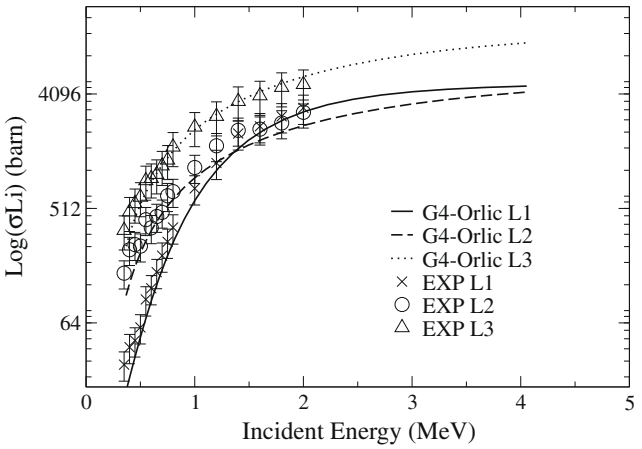

Fig. 12. L_i-subshell ionization cross sections of element Z_2 = 48.

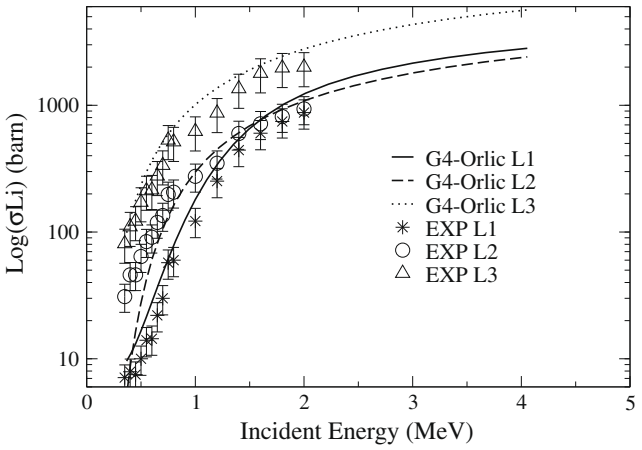

Fig. 13. L_i-subshell ionization cross sections of element $Z_2 = 52$.

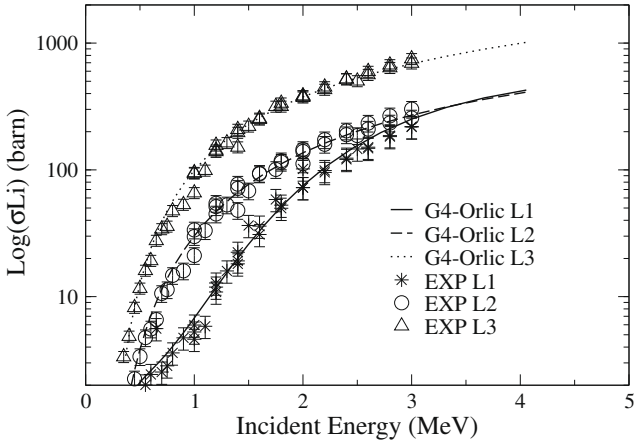

Fig. 14. L_i-subshell ionization cross sections of element $Z_2 = 66$.

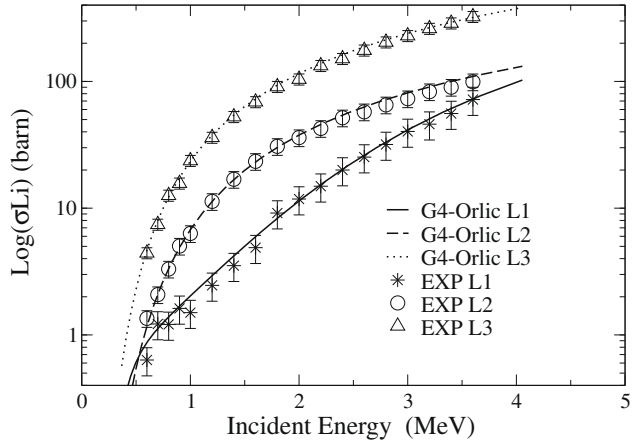

Fig. 15. L_i-subshell ionization cross sections of element $Z_2 = 75$.

For targets with low atomic number ($14 \leqslant Z_2 \leqslant 42$), only coefficients for total L-shell were obtained. Comparative results are shown in figures below, from Figs. 11–16. We plot L_i-subshell ionisation cross sections in logarithmic scale in order to show them on the same graphs.

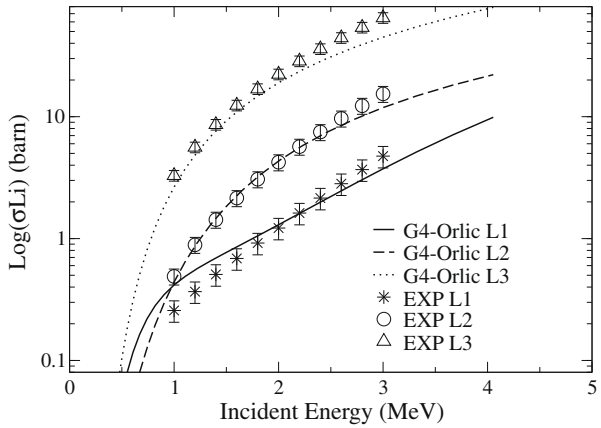

Fig. 16. L_i-subshell ionization cross sections of element $Z_2 = 90$.

5.5. Results and discussion

As can be seen from Fig. 11, experimental values and Geant4-semi-empirical results scatter for more than a factor of 2 for some incident energy values. In addition, according to almost all publications on total L ionisation cross sections within light elements ($Z_2 \leqslant 42$), experimental values deviate significantly from the theoretical predictions. None of the present theories gives satisfactory predictions that agree with experimental values for that atomic number range. Moreover, since there are no newly published total L ionisation cross sections for elements with $14 \leqslant Z_2 \leqslant 42$, the fitting coefficients given by Orlic et al. [55] are the same as those reported in their earlier work [53].

For the other five groups within $43 \leqslant Z_2 \leqslant 92$, the Geant4 implemented semi-empirical functions are, for all three subshells, close to the experimental data points. It is clear through figures Figs. 12–16 that our Geant4-implemented semi-empirical model for calculation of L_i-subshell ionisation cross sections gives good agreement for L_3 and L_2-subshell for all energies above 1 MeV (deviations are less then 10%). Below 1 MeV, it gives values lower than the experimental ones by 20–30%. The situation with L_1-subshell shows less agreement; experimental values are 10–30% higher than the semi-empirical ones for some energy values of the incident protons.

6. Conclusion

New classes for the computation of K and L_i-subshells ionisation cross have been implemented in the Low Energy Electromagnetic Package of Geant4 in order to improve the simulation of PIXE process. These classes are based on theoretical and semi-empirical calculation models. Comparative verification tests between the results obtained with Geant4 using these new classes and experimental cross sections have been presented and discussed. Geant4-results were divided into five and six groups according to the atomic number of target elements and each set was treated and compared with experimental values to evaluate the degree of discrepancy and/or agreement.

As expected, both of Geant4-ECPSSR theoretical model and Geant4-Paul's model produce values of K-shell ionisation cross sections in a relatively good agreement with experimental data. This agreement is noted similarly for protons and alpha particles projectiles. The two Geant4-implemented cross sections (*G4ecpssrCrossSection* and *G4PaulKCrossSection*) generally over-predicts experimental values of K-shell ionization cross sections by more than 10% for light target elements in the range $Z_2 \leqslant 30$ and that divergence is function of incident energy values.

The verification of the Geant4-implemented semi-empirical computation (*G4OrlicLCrossSection*) of L_1, L_2 and L_3-subshell ionisation

cross sections ensures that there are no significant differences between the experimental and predicted cross section values. An average deviation of empirical ionisation cross sections from the corresponding Geant4-values is ranging from 7% with L_2 subshell values to 32% with L_1-subshell values.

The validation of a whole PIXE experiment taking into account these new cross section calculation classes and including the generation of atomic de-excitation is currently in progress and will be the object of another publication.

Acknowledgements

We would like to thank the director of INFN-Genoa, Prof. Sandro Squarcia, as well as Dr. John Apostolakis, spokesperson of the Geant4 collaboration, for their strong funding and collaborative assistance. We express our acknowledgment to Dr. Giacomo Cuttone, INFN-LNS, for his great support.

H. Ben Abdelouahed warmly acknowledges the continuous support of Prof. A. Trabelsi, director of the CNSTN-Tunisia, all along the achievement of this work. Dr. M. Telmini is also acknowledged for fruitful discussions.

References

[1] R. Zeisler, V.P. Guinn, Nuclear Analytical Methods in the Life Sciences, Humana, Clifton, NJ, 1990.
[2] S. Morita, Int. J. PIXE 2(1) (1992) ix.
[3] S.A.E. Johansson, Nucl. Instr. and Meth. B 75 (1993) 589.
[4] Geant4 collaboration, IEEE Trans. Nucl. Sci. 53(1) (2006) 270.
[5] Geant4 collaboration, Nucl. Instr. and Meth. A 506 (2003) 250.
[6] J.F. Breismeister, MCNP, A General Monte Carlo N-Particle Transport Code, version 4C, Manual LA-13709-M, 2000.
[7] F. Salvat, J.M. Fernadez-Varea, E. Acosta, J. Sempaul, PENELOPE, A code system for Monte Carlo simulation of Electron and Photon transport, Rapport NEA/NSC/DOC, ISBN92-64-18475, 19, 2001.
[8] W.R. Nelson, H. Hirayama, D.W.O. Rogers, The EGS4 code system, Rapport SLAC-265, Standard Linear Accelerator Center, Standford, California, 1985.
[9] G. Booch (Ed.), Object-Oriented Analysis and Design with Applications, The Benjamin/Cummings Publishing Co., Menlo, CA, 1999.
[10] G. Cosmo, in: Proceedings of Computing in High Energy and Nuclear Physics, Beijing, China, 2001, p. 469.
[11] S. Chauvie, G. Depaola, V. Ivanchenko, F. Longo, P. Nieminen, M.G. Pia, in: Proceedings of CLHEP Conference, Beijing, China, 2001, p. 337.
[12] J. Apostolakis, S. Giani, M. Maire, P. Nieminen, M.G. Pia, L. Urban, Geant4 Low Energy Electromagnetic Models for electrons and photons, INFN/AE-99/18, Frascati, 1999.
[13] P. Rodrigues et al., IEEE Trans. Nucl. Sci. 51 (4) (2004) 1412.
[14] J. Moscicki, S. Guatelli, A. Mantero, M.G. Pia, Nucl. Phys. B 125 (2003) 327.
[15] A. Mantero, M. Bavdaz, A. Owens, A. Peacock, M.G. Pia, in: Proceedings of IEEE-NSS, Portland, Oregon, 2003.
[16] D. Cullen et al., EPDL97, the Evaluated Photon Data Library, 97 version, UCRL-50400, 6, 1997.
[17] S.T. Perkins et al., Tables and Graphs of Electron-interaction Cross Sections from 10 eV to 100 GeV Drived from the LLNL Evaluated Electron Data Library (EEDL), UCRL-50400, 31, 1997.
[18] A. Mantero, B. Mascialino, M.G. Pia, S. Saliceti, Geant4 Atomic Relaxation Models, in: American Nuclear Society Topical Meeting in Monte Carlo, Chattanooga, Tennessee, 2005.
[19] S.T. Perkins et al., Tables and Graphs of Atomic Subshell and relaxation Data Derived from the LLNL Evaluated Atomic Data Library (EADL), Z = 1-100, UCRL-50400, 30, 1997.
[20] M. Grysinsky, Phys. Rev. A 138 (1965) 336.
[21] A. Mantero, Development and validation of X-ray fluorescence simulation models for planetary astrophysics investigations, Ph.D. Thesis, University of Genoa, 2008.
[22] S. Giani et al., Geant4 simulation of energy losses of slow hadrons, INFN Report, Technical Report INFN/AE-99/20, 1999.
[23] H. Paul, J. Sacher, Atom. Data Nucl. Data Tables 42 (1989) 105.
[24] T. Mukoyoma, Int. J. PIXE 1 (1991) 209.
[25] D.D. Cohhen, M. Harrigan, Atom. Data Nucl. Data Tables 34 (1986) 393.
[26] R.S. Sokhi, Crumpton, J. Phys. B, Atom. Mol. Phys. 18 (1985).
[27] J.J. Thomson, Philos. Mag. 23 (1912) 449.
[28] G. Lapicki, Lect. Notes Phys. 294 (1988).
[29] J. Bang, J.M. Hansteen, Mat. -Fys. Medd. (1959) 1.
[30] E. Merzbacher, H.W. Lewis, E. Encyclopedia of physics, Vol. 34, Springer-Verlag, Berlin, 1958. P.166.
[31] G. Lapicki, Rad. Phys. Chem. 76 (2006) 475.
[32] Y. Awaya, T. Kambara, Y. Kanai, Int. J. Mass Spectrom. 192 (1999) 49.
[33] V. John Kennedy, A. Augusthy, K.M. Varier, P. Magudapathy, K.G.M. Nair, B.B. Dhal, H.C. Padhi, Nucl. Instr. and Meth. B 161–163 (2000) 196.
[34] O.G. de Lucio, J. Miranda, L. Rodriguez-Fermandez, K X-ray production by $^{12}C^{4+}$ ion impact on selected elements, Rad. Phys. Chem. 73 (2005) 189.
[35] Z. Smit, Nucl. Instr. and Meth. B 189 (2002) 1.
[36] R. Rice, G. Basbas, F.D. McDaniel, Atom. Nucl. Data 20 (1997) 503.
[37] W. Brandt, G. Lapicki, Phys. Rev. A 23 (1981) 1717.
[38] S.J. Cipolla, Z. Liu, Comput. Phys. Commun. 97 (1996) 315.
[39] Sam J.. Cipolla, Comput. Phys. Commun. 176 (2006) 157.
[40] J. Campbell, Atom. Data Nucl. Data Tables 85 (2003) 291.
[41] T.B. Akselsson, Zeit. fur. Physik 266 (1974) 245.
[42] T.B. Johansson, S.A.E. Johansson, Nucl. Instr. and Meth. B 137 (1976) 473.
[43] C.M. Romo-Kroger, Nucl. Instr. and Meth. B (1998) 136.
[44] H. Paul, Nucl. Instr. and Meth. B 3 (1984) 51.
[45] P. Cuzzocrea, E. Perillo, E. Rosato, G. Spadaccini, Vigilante, J. Phys. B: Atom. Mol. Phys. 18 (1985) 711.
[46] Y.C. Yu, C.W. Wang, E.K. Lin, T.Y. Liu, H.L. Sun, J.W. Chiou, G. Lapicki, J. Phys. B Atom. Mol. Opt. Phys. 30 (1997) 5791.
[47] S.J. Cipolla, Nucl. Instr. and Meth. B 261 (2007).
[48] M. Vigilante, P. Cuzzocrea, N. De Cesare, F. Murolo, E. Perillo, G. Spadaccini, Nucl. Instr. and Meth. B 51 (1990) 232.
[49] E. Braziewicz, L. Braziewicz, D. Trautmann, J. Phys. B Atom. Mol. Opt. Phys 24 (1991) 1669.
[50] T. Mukoyoma, L. Sarkadi, Phys. Rev. A 25 (1982).
[51] V.J. Kennedy, A. Augusthy, H.C. Padhi, Nucl. Instr. and Meth. (2000).
[52] G. Lapicki, Nucl. Instr. and Meth. B 189 (2002).
[53] I. Orlic, C.H. Sow, S.M. Tang, Atom. Data Nucl. Data Tables 56 (1994) 159.
[54] H. Sow, I. Orlic, S. Myagawa, Nucl. Instr. and Meth. B 75 (1993) 58.
[55] I. Orlic, C.H. Sow, S.M. Tang, Int. J. PIXE 4 (1994) 217.
[56] H. Paul, J. Muhr, Phys. Rep. 135 (1986) 47.